Environmental Technology

ISSN: 0959-3330 (Print) 1479-487X (Online) Journal homepage: www.tandfonline.com/journals/tent20

Characterization of adsorption of aqueous arsenite and arsenate onto charred dolomite in microcolumn systems

Yousef Salameh, Ala'a H. Al-Muhtaseb, Hasan Mousa, Gavin M. Walker & Mohammad N.M. Ahmad

To cite this article: Yousef Salameh, Ala'a H. Al-Muhtaseb, Hasan Mousa, Gavin M. Walker & Mohammad N.M. Ahmad (2014) Characterization of adsorption of aqueous arsenite and arsenate onto charred dolomite in microcolumn systems, Environmental Technology, 35:24, 3029-3040, DOI: 10.1080/09593330.2014.929181

To link to this article: https://doi.org/10.1080/09593330.2014.929181

Published online: 25 Jun 2014.

Environmental Technology, 2014
Vol. 35, No. 24, 3029–3040, http://dx.doi.org/10.1080/09593330.2014.929181

Characterization of adsorption of aqueous arsenite and arsenate onto charred dolomite in microcolumn systems

Yousef Salameh[a], Ala'a H. Al-Muhtaseb[b], Hasan Mousa[b,c], Gavin M. Walker[d,e] and Mohammad N.M. Ahmad[a,d*]

[a]*Department of Mechanical Engineering, Faculty of Engineering and Architecture, American University Beirut, Beirut, Lebanon;* [b]*Petroleum and Chemical Engineering Department, Faculty of Engineering, Sultan Qaboos University, Muscat, Oman;* [c]*Department of Chemical Engineering, Jordan University of Science and Technology, Irbid 22110, Jordan;* [d]*The QUESTOR Centre, School of Chemistry and Chemical Engineering, Queen's University Belfast, Belfast BT9 5AG, Northern Ireland, UK;* [e]*Department of Chemical and Environmental Sciences, Materials Surface Science Institute, University of Limerick, Limerick, Ireland*

(*Received 21 September 2013; final version received 21 May 2014*)

In this work, the removal of arsenite, As(III), and arsenate, As(V), from aqueous solutions onto thermally processed dolomite (charred dolomite) via microcolumn was evaluated. The effects of mass of adsorbent (0.5–2 g), initial arsenic concentration (50–2000 ppb) and particle size (<0.355–2 mm) on the adsorption capacity of charred dolomite in a microcolumn were investigated. It was found that the adsorption of As(V) and As(III) onto charred dolomite exhibited a characteristic 'S' shape. The adsorption capacity increased as the initial arsenic concentration increased. A slow decrease in the column adsorption capacity was noted as the particle size increased from >0.335 to 0.710–2.00 mm. For the binary system, the experimental data show that the adsorption of As(V) and As(III) was independent of both ions in solution. The experimental data obtained from the adsorption process were successfully correlated with the Thomas Model and Bed Depth Service Time Model.

Keywords: arsenic; dolomite; charred dolomite; microcolumn; adsorption; water treatment

1. Introduction

Arsenic pollution in the aquatic environment is a worldwide concern due to its toxicity and chronic effects on human health.[1] The chronic toxicity of arsenic in drinking water is known to cause several health problems such as cancer, harming the central and peripheral nervous systems and causing serious skin problems and reproductive disorders.[2] High concentrations of arsenic in natural water have been reported in many areas all over the world such as Bangladesh, China, India, Taiwan, Japan, Serbia, Canada, United States, Argentina, Mexico and Chile.[3] Arsenic reaches water supplies as a result of natural processes such as weathering reactions, biological activity and volcanic emission [4] as well as a consequence of anthropogenic impacts such as oil and coal burning power plants, waste incineration, cement works, disinfectants, ore production and processing, metal treatment, wood preservatives, pesticides, oil and solvent recycling.[5] Arsenic generally occurs as arsenate (As(V)) and arsenite (As(III)). As(III) is considered more toxic than As(V) and tends to be more mobile in the environment.[6] As(V) species occurs mainly in the form of H_2AsO_4 in the pH range between 3 and 6, while a divalent anion $HAsO_4^{2-}$ dominates at higher pH values (such as between pH 8 and 11). In the intermediate region, which is in the pH range between 6 and 8, both species coexist with one another.[7] Thus, it is evident that in the pH range of natural waters, As(V) remains in the anionic state which is highly favourable for adsorption.[8] Compared with As(V), As(III) removal mechanism is somewhat more complicated. This is due to the fact that As(III) is stable as neutral H_3AsO_3 at pH <9. As a result, As(III) adsorption is quite independent with change in pH of solution from 3 to 9.

Various treatment technologies to remove arsenic from drinking water have been designed such as: coagulation; ion exchange; reverse osmosis; liquid–liquid extraction and adsorption.[9,10] However, in many areas of the world there is still in a necessity for appropriate technologies, which are inexpensive, simple to use and easily applied to source use. Various adsorbents for arsenic removal have been developed that include materials such as ferrihydrite,[11] metallic iron nanoparticles,[12] volcanic ash,[13] biomass [14] and titanium dioxide nanotube arrays.[15]

Dolomite, which represents a potential low-cost adsorbent,[16] is a common sedimentary rock-forming mineral that can be found in sedimentary beds several hundred feet thick; it is also found in metamorphic marbles, hydrothermal veins and replacement deposits.[17] The Dolomite Group is composed of minerals with an unusual trigonal bar 3 symmetry. The general formula of this group

*Corresponding author. Email: mnm.ahmad@qub.ac.uk

is $AB(CO_3)_2$, where A can be either calcium, barium or strontium and the B can be either iron, magnesium, zinc or manganese. The amount of calcium and magnesium in most specimens is equal, but occasionally one element may have a slightly greater presence than the other. Small amounts of iron and manganese are sometimes also present.[18,19] The majority of the industrial applications of dolomite require a thermal treatment process. This thermal processing is accompanied by structural changes within the solid product, causing a significant change in the crystallographic, morphological and textural properties. Obviously, the modification in the interfacial properties of dolomitic solids will improve their adsorption properties.[20]

Adsorption process can be performed under either a batch or continuous mode. For a continuous process, a microcolumn is usually used. However, adsorption capacities from batch studies, although useful, may not provide accurate scale-up information.[21] From the industrial point of view, column system is very practical because of the low reagent handling, adaptability of column systems to multipurpose processes and low operational costs.[22] Li et al. [6] stated that the microcolumn technique can acceptably simulate the bed performance for large column trials.

To our knowledge, there is no research in the literature related to the use of microcolumns to study the adsorption behaviour of arsenic onto dolomite and thermally modified dolomite (charred). Therefore, the aim of this work was to investigate the adsorption capacity of charred dolomite for the removal of As(V) and As(III) in microcolumns. The effect of initial arsenic concentration, adsorbent particle size and adsorbent dose was also studied. For an accurate design of an adsorption column, an accurate prediction of the breakthrough curve of the effluent concentration (or the concentration–time profile) is needed. Therefore, the experimental results obtained from the continuous system were fitted to the Thomas model and the Bed Depth–Service Time (BDST) model.

2. Materials and methods

2.1. *Dolomite and charred dolomite*

Dolomite used in this work was mined in Belcoo, County Fermanagh, Northern Ireland (UK) and grounded into different particle sizes. The typical chemical composition of the dolomite in the deposit was 44 wt% $MgCO_3$ and 53 wt% $CaCO_3$. Preliminary experiments were conducted to evaluate the impact of using raw dolomite as an adsorbent for As(V) and As(III). However, the results indicated a very low removal. Therefore, the dolomite was activated thermally under different temperatures. A Carbolite-type RHF 14/4 furnace was used to char the dolomite at the following temperatures: 600 °C, 700 °C and 800 °C. The crucibles were filled with approximately 10 g of dolomite and placed into the furnace, which was heated to the required temperature for the allotted time (1, 2, 4 and 8 h), after which the furnace was turned off and left open for few hours to cool down and then the samples were removed. The product was sieved to different particle sizes. The samples were left in the furnace during the heating and cooling of the furnace to prevent the sudden heating or cooling, which would affect the structure of the particles. The samples weight was measured before and after the charring process to determine the percentage of weight loss in each.

Preliminary results show that the maximum removal takes place on the samples which have been charred to 800 °C, but this charred dolomite was found inapplicable since it is dissolved in the solution during the process; this can be attributed to the fact that the magnesium carbonate component of the dolomite decomposes at temperatures around 800 °C.[23] The decomposition of dolomite at 800 °C leads to changes in the chemical composition of the surface and weakens the porosity of the mineral. The efficiency of the dolomite at 700 °C for 8 h was found to be almost as much as the efficiency of the dolomite at 800 °C. Therefore, the study was conducted on the dolomite at 700 °C for 8 h.

2.2. *Adsorbates*

The standard stock solutions of As(V) and As(III) were prepared by appropriate dilution with deionized water to a final concentration of 5000 ppb. As(V) stock solution was prepared from sodium arsenic dibasic heptahydrate ($Na_2HAsO_4 \cdot 7H_2O$; Aldrich Chemical Co., Inc. USA). As(III) stock solution was prepared from sodium arsenite ($NaAsO_2$; Aldrich Chemical Co., Inc., USA). In addition, 0.1 g $NaHCO_3$ was added to buffer pH fluctuations during the experiment. Most ground waters have some amount of alkalinity present, which tends to be in the order of 250–600 mg/L HCO_3. The addition of bicarbonate is, therefore, not seen to compromise the experiments.

2.3. *Surface area*

The surface area of the samples was determined using the N_2 gas adsorption method. Nitrogen adsorption isotherms of the adsorbents were determined at 77 K using gas adsorption apparatus, Quantachrome instruments NOVA *e*-Series. The weight of the samples was approximately 0.4 g. All the samples were outgassed under vacuum at 100 °C for 24 h in a vacuum system at about 1 atm, before nitrogen adsorption takes place.

2.4. *X-ray diffraction (XRD)*

To identify the structure and determine the compositions of raw and charred dolomite, XRD analysis was carried out using Siemens Diffractometer D 5000 with Cu Kα radiation ($\lambda = 0.15418$ nm, 40 kV and 40 mA). The sample was scanned from 20° to 80° (2θ) at a rate of 0.02°/min. The XRD of fresh and spent adsorbent was carried out in which adsorbent spent samples were removed from the arsenic solution after equilibration and freed from the water by drying at 65 °C. Qualitative analyses of the data were performed using Diffrac-AT version 3 software by Scobain Siemens and JCPDS data files. Quantitative analysis of the XRD data was conducted using SIRQUANT Quantitative XRD software.

2.5. Microcolumn experiment

The column tests were carried out in a microglass column with an inside diameter of 9.14 mm. The microcolumns were filled with various dolomite samples. Air pockets may form in the column, which could lead to channelling, increase in pressure drop and premature breakthrough, due to the air pockets reducing the surface available for mass transfer between the dolomite and the arsenic solution. To solve this problem, deionized water was used to wash the sample to remove air bubbles and to rinse the dolomite. A predetermined mass of dry dolomite particles was filled in the microcolumn soaked with deionized water for approximately 15 min to eliminate air pockets form in the column. After this de-aeration step, arsenic solution was continuously fed to the top of the column at a steady-flow rate controlled by a peristaltic pump (Watson-Marlow, 101U) connected with Teflon tubes to the column inlet until breakthrough occurs. The columns were kept in vertical position. Samples were taken at regular intervals, normally every 15 min, filtered through a 0.45-µm cellulose nitrate membrane filter (Swinnex-25 Millipore) and prepared for analyses using inductively coupled plasma (ICP), Perkin-Elmer 400. The samples were prepared up to 10 mL to give a 2% nitric acid solution. Duplicate samples were measured and standard error in the readings was smaller than 3%. Stock solutions of As(V) and As(III) were prepared with a concentration of 5000 µg/L. Concentrations of 50, 500 and 2000 µg/L were prepared for As(V) and As(III) by diluting the stock solutions with deionized water. Before starting the adsorption tests, the system was checked by circulating water. The main components of the system are: (i) peristaltic pump, (ii) microcolumn, (iii) Teflon tubes and (iv) glass wool. The details of experimental conditions of the microcolumn studies of arsenic onto charred dolomite for the entire microcolumn runs undertaken are listed in Table 1. To study the affinity of As(V) and As(III) for charred dolomite in the microcolumn studies, single-component and binary component adsorption experiments were also carried out. All experiments were conducted at a room temperature of 22 °C. Duplicate samples were measured and the standard error in the readings was smaller than 3%.

2.6. Modelling of column data

The fixed-bed performance is conveniently described through the concept of the adsorption breakthrough curve.[24] The breakthrough curves are found by plotting throughput volume (V) at any time (t) *versus* effluent (arsenic) concentration (C). For our calculations, the breakthrough time was defined as the time for effluent reaching $C_t/C_0 = 0.95\%$ for a feed. Throughput volume was calculated using:

$$V = F \times t_{\text{total}} \tag{1}$$

where F is the volumetric flow rate (L/min) and t_{total} is the total flow time (min).

Two mathematical models have been applied for the experimental data to predict the dynamic behaviour and the performance of the fixed-bed column.

2.6.1. Thomas model

The Thomas equation is one of the most general and widely used methods to predict the adsorption process. It was derived based on the following theory: Langmuir adsorption/desorption; no axial dispersion and the rate driving force follows second-order reversible reaction kinetics [25]:

$$\frac{C_t}{C_0} = \frac{1}{1 + \exp[(k_T/F)(q_0 m - C_0 V)]} \tag{2}$$

$$\Rightarrow \ln\left(\frac{C_0}{C_t} - 1\right) = \frac{k_T q_0 m}{F} - \frac{k_T C_0}{F} V \tag{3}$$

where C_0 is the initial arsenic concentration (µg/L), C_t is the equilibrium concentration (µg/L) at time t(min),

Table 1. Experimental conditions of the various microcolumn adsorption experiments for the removal of arsenic onto charred dolomite.[a]

	Variables		
Parameters studied	Initial arsenic concentration (µg/L)	Mass of adsorbent (g)	Particle size (mm)
Mass of adsorbent (g)	500	0.5, 1, 2	0.710–2.00
Particle size (mm)	500	1	<0.355, 0.355 − 0.710, 0.710 − 2.00
Initial arsenic concentration (µg/L)	50, 500, 2000	1	0.710–2.00

[a]Flow rate = 1.1 mL/min; internal diameter = 9.14 mm.

k_T is the Thomas constant (L/min μg), F is the volumetric flow rate (L/min), q_0 is the maximum column adsorption capacity (μg/g), m is the mass of adsorbent (g) and V is the cumulative throughput volume (L). It can be noted from the definition of the Thomas constant that it has an inverse relationship with the amount of adsorption. A plot of $\ln(C_0/C_t - 1)$ versus V gives a straight line with a slope of $(-k_T C_0/F)$ and an intercept of $(k_T q_0 m/F)$.

2.6.2. Bed depth-service time model (BDST)

The BDST model is generally exploited for the evaluation of different column design parameters with the assumption that the rate of adsorption is controlled by the surface reaction between adsorbate and the unused capacity of the adsorbent. If the adsorption zone is moving at a constant speed along the column, the bed adsorption capacity, N_0, will be constant throughout the bed. With these assumptions, the BDST model provides useful modelling equations for the changes of system parameters such as flow rate and initial feed concentration.[26]

The linear relationship between bed depth, Z, and service time, t, is

$$\ln\left(\frac{C_0}{C_b} - 1\right) = \ln(e^{K_a N_0 Z/F} - 1) - K_a C_0 \cdot t \tag{4}$$

where C_0 is the initial arsenic concentration (μg/L), C_b is the breakthrough arsenic concentration (μg/L), Z is the bed depth (dm), N_0 is the column adsorption capacity in BDST model (g/L), F is the flow rate (L/min) and K_a is the adsorption rate constant (L/g min).

Because the exponential term is usually much higher than unity, the unity term within the brackets on the left-hand side of equation is often neglected

$$e^{K_a N_0 Z/F} >> 1 \Rightarrow \ln\left(\frac{C_0}{C_b} - 1\right) = \left(\frac{K_a N_0 Z}{F}\right) - K_a C_0 t \tag{5}$$

Therefore, the linear relationship between the bed depth, Z, and the service time at breakthrough, t_B, is

$$t_B = \left(\frac{N_0}{C_0 F}\right) Z - \frac{1}{K_a C_0} \ln\left(\frac{C_0}{C_b} - 1\right) \tag{6}$$

$$\Rightarrow t_B = aZ + b \tag{7}$$

where a is the slope and b is the intercept of the equation.

After identifying a and b, Equation (6) becomes a simple relationship between the service time at breakthrough and the bed depth (Equation 7). A group of straight lines of t_B versus Z can be plotted, each line corresponding to a fixed value of C_0/C_b (i.e. a fixed percentage removal).

3. Results and discussion

3.1. XRD analysis

X-ray diffraction analyses were carried out to verify the quality of the dolomite. Figure 1(a) shows the powder XRD pattern of crushed untreated dolomite. All the peaks in Figure 1(a) represent the dolomite. Figure 1(b) depicts the powder XRD pattern of charred dolomite at 700 °C for 8 h. The XRD data show a trace of magnesium oxide, which is a proof that charring the dolomite at 700 °C for 8 h is sufficient to cause the dissociation of some magnesium carbonate to magnesium oxide. There is also a small presence of calcium hydroxide, which may be a result of the grinding procedure when partial decomposition of dolomite may have occurred. But this is not supported by the XRD data for the raw crushed dolomite in Figure 1(a), which shows no indication of calcium hydroxide being present. It may be the case that while the temperature is not sufficient to cause the thermal dissociation of $CaCO_3$ in the bulk particles, it may be sufficient to cause the partial dissociation of the fine dolomite particles resulted from grinding on the surface of the dolomite. It requires less input of energy to dissociate the $CaCO_3$ in the fine particles due to the energy dissipated as heat during the grinding process. This indicates that the MgO formed is insufficiently reactive to form magnesium hydroxide with the water vapour present in the air.

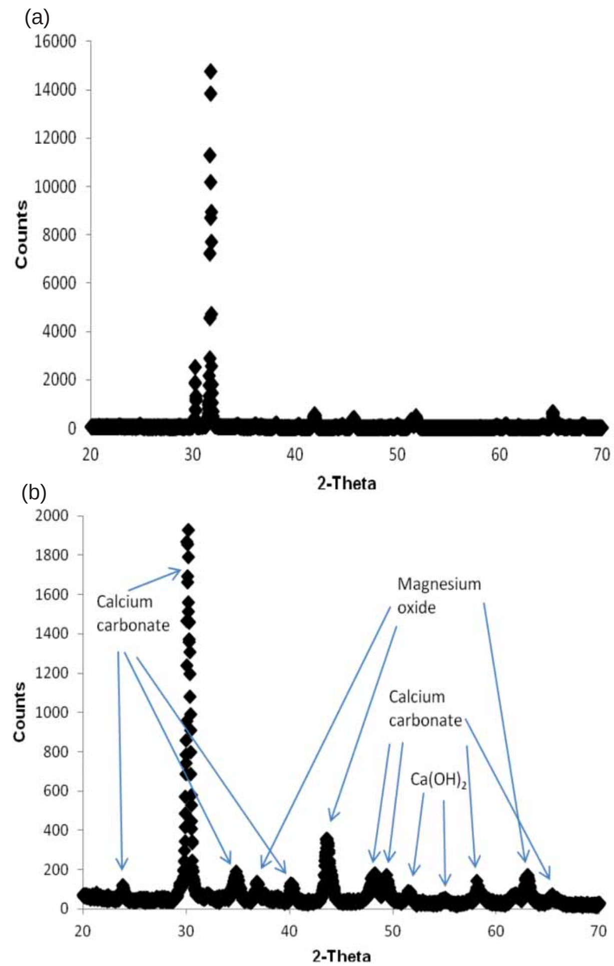

Figure 1. XRD pattern of (a) raw dolomite and (b) charred dolomite at 700 °C for 8 h.

Table 2. Surface areas of raw and charred dolomite.

Sample	BET surface area (m^2/g)
Raw dolomite	0.89
600 °C for 1 h	1.32
600 °C for 2 h	2.45
600 °C for 4 h	3.58
600 °C for 8 h	3.95
700 °C for 1 h	2.83
700 °C for 2 h	3.41
700 °C for 4 h	5.73
700 °C for 8 h	7.31
800 °C for 1 h	5.60
800 °C for 2 h	6.15
800 °C for 4 h	10.86
800 °C for 8 h	11.81

3.2. Surface area

Table 2 shows the BET surface area of raw dolomite and dolomite charred at different temperatures. It can be seen that the charring procedure has a significant effect on the cumulative surface area. It indicates that the surface area of the selected charred dolomite at 700 °C (8 h) is eightfold higher than that for the raw material, which means that more area is available for the adsorption of the arsenic ions onto the charred dolomite.

3.3. Effect of initial arsenic concentration

The effect of initial arsenic concentration on the shape of the breakthrough curves and the column adsorption parameters was studied. Figure 2(a) and (b) depicts the breakthrough curves of the adsorption of arsenic onto dolomite and charred dolomite at different initial arsenic concentrations as a plot of dimensionless concentration (C_e/C_0) versus volume (V) of arsenic solution treated. It can be seen from Figure 2(a) and (b) that the shape of the breakthrough curves of adsorption of As(V) and As(III) onto charred dolomite at various initial arsenic concentrations exhibited a characteristic 'S' shape. The initial arsenic concentration is important since a given mass of dolomite can only adsorb a certain amount of the adsorbate. As expected, with more concentrated solutions, a smaller volume of solution can be treated before column breakthrough, as all the available adsorption sites will be occupied more rapidly. It is shown that increasing the inlet arsenic concentration at constant flow rate decreased the throughput volume until the breakthrough time ($C_e/C_0 = 0.05$). This can be attributed to the high arsenic concentrations saturating the active adsorption sites within the dolomite more rapidly, thus decreasing the breakthrough time. Exhaustion of the adsorption bed is assumed to have occurred when the effluent concentration is equal to 95% of the influent concentration.[27]

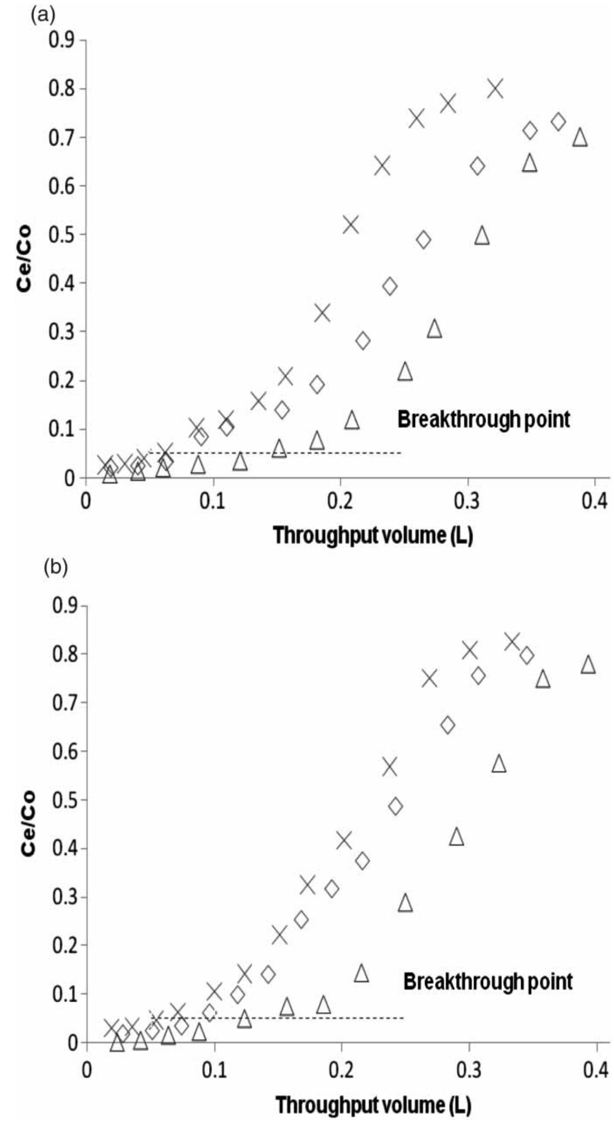

Figure 2. Breakthrough curves for the adsorption of (a) As(V) onto charred dolomite and (b) As(III) onto charred dolomite using microcolumn at different initial arsenic concentrations. Mass of dolomite and charred dolomite: 1 g; internal diameter: 9.14 mm; flow rate: 1.1 mL/min (Δ: 50 ppb, ◇: 500 ppb, x: 2000 ppb).

Thomas equation was used to estimate the column adsorption parameters: k_T (Thomas constant) and q_0 (maximum column adsorption capacity). Table 3 summarizes the adsorption parameters. The values of the correlation coefficient (R^2) indicate that the experimental data are well presented by the Thomas equation over a wide range of the arsenic concentration. It is shown that the adsorption capacity increased as the initial arsenic concentration increased. Higher initial arsenic concentrations lead to a higher concentration gradient so the mass transfer driving force will be higher. It is also noted that the adsorption capacity of the charred dolomite for the As(V) is higher than adsorption capacity for As(III). This may be due to the formation of

Table 3. Thomas parameters for the adsorption of arsenic using microcolumn at different arsenic initial concentrations.

Concentration	k_T (mL/min µg)	q_0 (µg/g)	R^2
As(V) onto charred dolomite			
50 ppb	339.2×10^{-3}	16.28	0.991
500 ppb	31.8×10^{-3}	139.58	0.986
2000 ppb	9.9×10^{-3}	437.15	0.984
As(III) onto charred dolomite			
50 ppb	410.2×10^{-3}	15.27	0.973
500 ppb	38.8×10^{-3}	123.56	0.990
2000 ppb	9.6×10^{-3}	433.90	0.993

arsenic oxide and arsenic carbonate (possibly by precipitation of the latter) from As(V), as this has a stronger positive charge than the As(III) over the neutral pH range.

Table 3 also shows that the rate constant, k_T, decreases as the initial arsenic concentration increases. The increase in arsenic concentration results in an increase in the driving force, which will enhance the diffusion of arsenic molecules onto dolomite pores. k_T values for the As(V)–charred dolomite system are smaller than those for the As(III)–charred dolomite system, which displays the higher affinity of this adsorbent to As(V).

The thermal treatment of the dolomite has clearly improved the uptake of As(V) and As(III). This can be attributed to the fact that the thermal treatment of dolomite leads to the transition to a mixture of calcite and magnesium oxide (causing an increase in the oxide content in the resulting solid). This increases the number of positively charged sites available inside these solids and raises the possibility of formation of arsenic oxide and arsenic carbonate and the precipitation of the latter one.

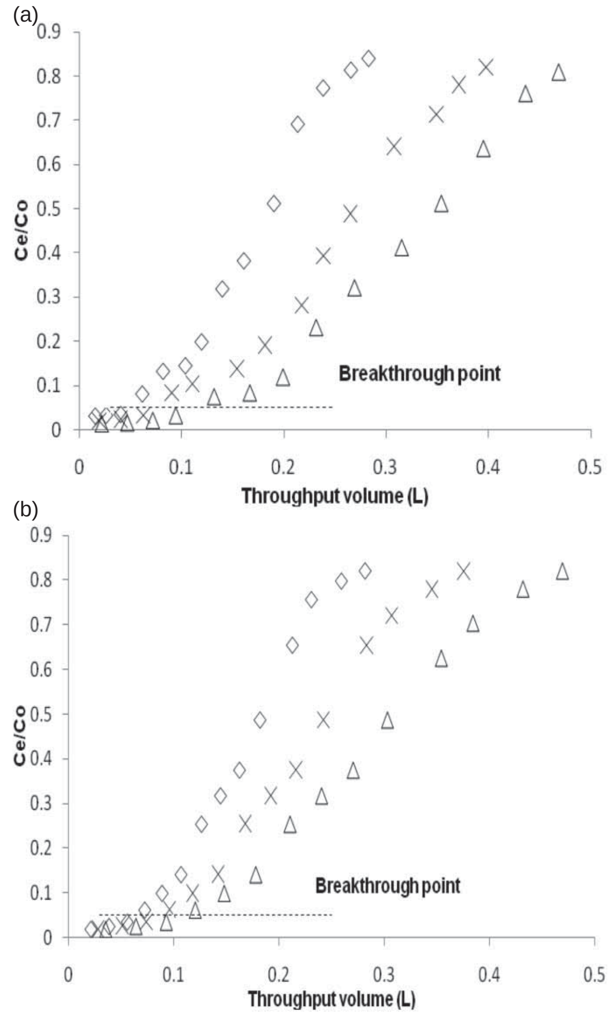

Figure 3. Breakthrough curves for the adsorption of (a) As(V) onto charred dolomite, (b) As(III) onto charred dolomite using microcolumn at various masses of dolomite. The concentration of As(V): 500 ppb; concentration of As(III): 500 ppb; internal diameter: 9.14 mm; flow rate: 1.1 mL/min (Δ: 2 g, x: 1 g, ◇: 0.5 g).

3.4. *Effect of adsorbent mass*

The observed breakthrough curves of arsenic adsorption onto dolomite at three different masses of adsorbent are displayed in Figure 3(a) and (b), plotted as the effluent concentration ratio versus the throughput volume. It is clear that the shape of the breakthrough curves for As(V) and As(III) onto various masses of charred dolomite is different. All the curves exhibited a characteristic 'S' shape. Figure 3(a) and (b) also indicates that the breakthrough curves moved towards the *y*-axis with decreasing mass of adsorbent. Correspondingly, the time needed to reach breakthrough increased as the mass of the adsorbent increased. The removal of As(V) and As(III) increased with the increase in the charred dolomite mass from 0.5 to 2 g. The increase in the arsenic uptake capacity with the increase in the adsorbent mass in the column can be attributed to increased adsorbent surface area available for the arsenic chemisorption, also higher concentrations of $MgCO_3$ and $CaCO_3$, which would increase the probability of formation arsenic oxide and arsenic carbonate, thus increasing in the extent of precipitation as a mechanism of arsenic removal.[28] Essentially, the lower the mass of adsorbent to be used, the smaller the volume of the solution that can be treated before breakthrough.

As can be observed in Figure 3(a) and (b), at the lowest mass of adsorbent, i.e. 0.5 g, a relatively lower uptake value was observed for arsenic at the beginning of column adsorption. In addition, as the arsenic solution continued to flow, the As(V) and As(III) concentrations in the effluents rapidly increased, as the adsorbent beds became saturated with arsenic molecules. Less sharp breakthrough curves were obtained at higher mass of adsorbent. The variation in breakthrough curve shape with dolomite mass is mainly due to the variations in the length of the adsorption zone, i.e. the particles of dolomite near the bottom of the adsorption column come into contact with arsenic solution before the particles near the top of column are exhausted. Also,

Table 4. Thomas parameters for the adsorption of arsenic using microcolumn at various masses of dolomite.

Mass of adsorbent	k_T (mL/min μg)	q_0 (μg/g)	R^2
As(V) onto charred dolomite			
0.5 g	43.4×10^{-3}	93.12	0.986
1 g	31.3×10^{-3}	137.94	0.989
2 g	27.8×10^{-3}	172.75	0.992
As(III) onto charred dolomite			
0.5 g	47.0×10^{-3}	94.98	0.983
1 g	34.7×10^{-3}	127.4	0.981
2 g	27.6×10^{-3}	160.61	0.986

the mass transfer zone is dependent upon the nature of adsorbent–adsorbate interactions.

Thomas equation was used to estimate the variation in the column adsorption parameters (k_T and q_0) with the variation in the dolomite mass. Table 4 summarizes the adsorption parameters. The experimental data are well presented by the Thomas equation over a wide range of the arsenic concentration with R^2 ranging from 0.986 to 0.992 for As(V) onto charred dolomite and 0.981 to 0.986 for As(III) onto charred dolomite. It is shown that the adsorption capacity increased as the mass of the dolomite increased in all the adsorption processes studied. A higher dolomite mass will lead to a higher concentration gradient; therefore, the mass transfer driving force will be higher. The adsorption capacity of the charred dolomite for the As(V) is higher than the adsorption capacity for As(III).

Table 4 also shows that the rate constant, k_T, decreases as the mass of dolomite increases. The increase in dolomite mass results in an increase in the adsorbent surface area available for the arsenic chemisorption, also higher concentrations of $MgCO_3$ and $CaCO_3$, which would increase the probability of formation of arsenic oxide and arsenic carbonate. k_T values for the As(V)–charred dolomite system are smaller than those for the As(III)–charred dolomite system, which displays the higher affinity of this adsorbent to the charred dolomite.

The analysis of the experimental breakthrough data using the BDST equation yielded a plot of bed depth, Z, versus service time, t_s. The linearization of the experimental data using this mathematical model was successful for the adsorption of arsenic onto dolomite. However, a close examination of the straight lines suggests that the experimental points of the BDST deviate from a theoretical straight line. This behaviour may be due to the fact that the main assumption in the BDST model is that the adsorbate is adsorbed on the adsorbent surface immediately such that there is no diffusion problem.[25] Consequently, when the bed depth increases, the residence time of the arsenic solution inside the column increases and the arsenic molecules can diffuse deeper inside the adsorbent.

The aim of operating a column adsorption system is to achieve a breakthrough value, which is a certain degree of reduction in the arsenic concentration in the effluent. A low breakthrough value would mean having a low arsenic concentration in the effluent. Hence, increasing the breakthrough arsenic concentration will increase the volume of arsenic solution treated and the adsorbent would run longer. The value of the breakthrough arsenic concentration should not affect the slope of the BDST plots, i.e. the breakthrough curves are steep and the mass-transfer zone is very short.[25] In Tables 5 and 6, BDST data represent the evolution of the bed operating time (for different concentrations C_t = 20%, 40%, 60% and 80%) as a function of the bed depth (Z). Based on the experimental data obtained at different masses of adsorbent for the adsorption of arsenic onto dolomite, plotting time for 20%, 40%, 60% and 80% of the breakthrough against the bed depth gives a linear relationship (figures are not shown here) with high correlation coefficients. The BDST parameters, namely, BDST adsorption capacity, N_0, and rate constant, K_a, were calculated from the linearized experimental data and are presented in Tables 5 and 6, for 20%, 40%, 60% and 80% breakthrough. In these tables, the effect of percentage breakthrough value on the adsorption capacity is demonstrated for a fixed initial arsenic concentration.

The BDST adsorption capacity, N_0, provides a convenient way of describing the performance of an adsorbent, with high performance and efficient use of adsorbent characterized by high BDST adsorption capacities. In this work, the usual units of N_0 (μg/dm^3) have been recalculated using the bulk density of dolomite to provide an adsorption

Table 5. BDST parameters for As(V) adsorption onto charred dolomite.

	Service time at breakthrough percentages (min)						
Bed depth (mm)	20%	40%	60%	80%	N_0 (mg/dm^3)	N_0^a (μg/g)	K_a^b (L/μg min)
					20% ⇒ 41.3	47.70	–
8.50	158	219	267	340	40% ⇒ 71.2	82.33	–
14.90	174	227	279	362	60% ⇒ 97.5	112.74	3.21×10^{-6}
30.35	178	247	306	385	80% ⇒ 107.8	124.61	8.47×10^{-6}

[a] N_0 (μg/g) was calculated by multiplying the value of N_0 (mg/dm^3) by the bulk density.
[b] Values of K_a did not compute for 20% and 40% breakthrough due to their negative values.

Table 6. BDST parameters for As(III) adsorption onto charred dolomite.

Bed depth (mm)	Service time at breakthrough percentages (min) 20%	40%	60%	80%	N_0 (μg/dm^3)	N_0^{a} (μg/g)	K_a^{b} (L/μg min)
					20% ⇒ 40.9	47.27	–
8.50	161	222	272	342	40% ⇒ 65.2	75.37	–
14.90	173	230	280	361	60% ⇒ 89.6	103.57	3.15×10^{-6}
30.35	179	248	307	386	80% ⇒ 106.7	123.41	8.45×10^{-6}

[a] N_0 (μg/g) was calculated by multiplying the value of N_0 (mg/dm^3) by the bulk density.
[b] Values of K_a did not compute for 20% and 40% breakthrough due to their negative values.

capacity in terms of (μg/g). It is shown that the adsorption capacity increased as the breakthrough value increased in all the studied adsorption systems. As concluded earlier from Thomas equation, the adsorption capacity of the charred dolomite for As(V) is higher than the adsorption capacity for As(III). The calculated column adsorption capacity from the Thomas equation is higher than the value obtained by BDST model; however, this can be attributed to the fact that the BDST adsorption capacities were obtained at 20%, 40%, 60% and 80% breakthrough, while for the Thomas equation, the breakthrough was 100%. Tables 5 and 6 also show that the adsorption rate constant, K_a, increases as the breakthrough value increases in all the studied adsorption systems. K_a values for the As(V)–charred dolomite system are close to those for the As(III)–charred dolomite system. It is clear that the experimental data correlated well with the calculated data using the Thomas and the BDST equation. Therefore, it might be concluded that the Thomas and the BDST equations can produce accurate prediction for various arsenic concentration and mass of the dolomite. The reported results of the BDST analysis herein can be of great importance for designing adsorption column for treating wastewater from arsenic.

3.5. *Effect of particle size*

The column adsorption studies on the arsenic were carried out on charred dolomite of particle sizes <0.335, 0.335–0.710 and 0.710–2.00. The breakthrough curves of the three particle sizes for the three investigated systems are illustrated in Figure 4(a) and (b). As shown, an increase in the particle size increases the sharpness of the breakthrough curve. A smaller particle size will have a better adsorption performance. This is due to an increase in the external surface area and the number of active pores per unit mass of the adsorbent found with decreasing particle size. The crushing of the large particles to form smaller particles also facilitates crack formation, which further increases the surface area available for mass transfer. However, the data indicate that the mechanism of arsenic adsorption onto dolomite does not depend on the adsorbent particle size alone because of the small effect of the particle size variation

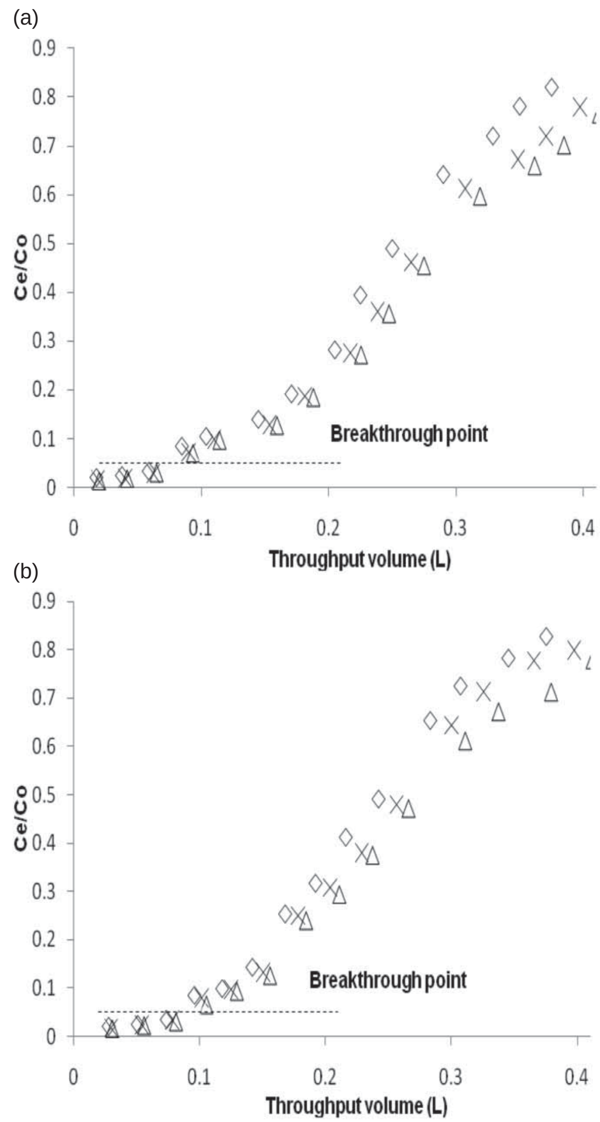

Figure 4. Breakthrough curves for the adsorption of (a) As(V) onto charred dolomite, (b) As(III) onto charred dolomite using microcolumn at various particle sizes of dolomite. Concentration of As(V): 500 ppb; concentration of As(III): 500 ppb; internal diameter: 9.14 mm; flow rate: 1.1 mL/min (Δ: $dp <$ 0.335 mm, x: 0.335 mm $< dp <$ 0.710 mm, ◇: 0.710 $< dp <$ 2.0 mm).

Table 7. Thomas parameters for the adsorption of arsenic using microcolumn at different particle sizes of dolomite.

Particle size	k_T (mL/min µg)	q_0 (µg/g)	R^2
As (V) onto charred dolomite			
$dp < 0.335$ mm	29.7×10^{-3}	151.94	0.980
0.335 mm $< dp < 0.710$ mm	30.5×10^{-3}	145.09	0.982
0.710 mm $< dp < 2.0$ mm	32.6×10^{-3}	131.31	0.989
As (III) onto charred dolomite			
$dp < 0.335$ mm	31.1×10^{-3}	146.27	0.972
0.335 mm $< dp < 0.710$ mm	32.9×10^{-3}	136.57	0.978
0.710 mm $< dp < 2.0$ mm	34.7×10^{-3}	126.47	0.982

in the amount of arsenic adsorbed; the increase in capacity with the decrease in particle size range suggests that arsenic does not completely penetrate the particle.

Moreover, the Thomas equation was used to estimate the rate constant and the adsorption capacity of the adsorption systems. Table 7 illustrates that the Thomas rate constant, k_T, increases with the increase in the mean adsorbent particle size. The crushing of the large particles to form smaller particles facilitates crack formation, which increases the surface area available for mass available for the arsenic chemisorptions. Furthermore, the adsorption capacity for the larger particle size is lower than that for smaller one. A small decrease in the column adsorption capacity with an increase in particle size in addition to the shift of the breakthrough curves was obtained resulting from an increase in the particle size from smaller than 0.335 mm to 0.710–2.00 mm. That behaviour can be attributed to the higher surface area of the smaller particle size; hence, a higher adsorption capacity is expected.

3.6. *Multicomponent adsorption*

The adsorption of a single arsenic component is not a common process in the wastewater treatment course. Wastewater effluent normally contains multi-species of arsenic with various concentrations and flow rates. In fact, little research has been published on the effect of multi-species adsorption in column systems. Competitive adsorption of As(V) and As(III) with a ratio of 1:1 onto different concentrations of charred dolomite using microcolumns was investigated and the results are illustrated in Figure 5. The figure shows that the adsorption of As(V) and As(III) increases with the increase in the charred dolomite concentration. Comparing the results with the results of the single-component systems, the adsorption of As(V) and As(III) was almost not affected by the presence of other molecules.

By a quick comparison of the breakthrough curve of the adsorption of single arsenic species with a mixture of As(V) and As(III) onto charred dolomite, it is apparent that the time that was spent to treat a fixed volume of multicomponent stream was almost the same in the case of a single-component stream. In other words, the presence of As(V) and As(III) in the mixture did not slow down the adsorption

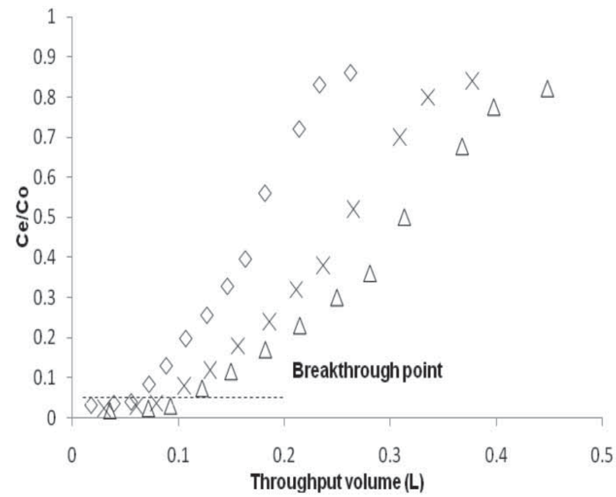

Figure 5. Breakthrough curves of adsorption of a mixture of As(V) and As(III) onto charred dolomite using microcolumn at various masses of charred dolomite. Concentration of mixture: 500 ppb; internal diameter: 9.14 mm; flow rate: 1.1 mL/min (Δ: 2 g, x: 1 g, ◇: 0.5 g).

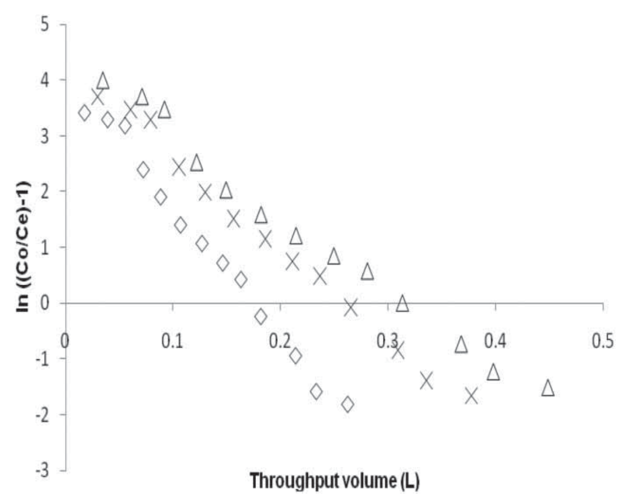

Figure 6. Thomas plot for adsorption of As(V) and As(III) mixture onto charred dolomite using microcolumn at various masses of dolomite (Δ: 2 g, x: 1 g, ◇: 0.5 g).

Table 8. Thomas parameters for the adsorption of As(V) and As(III) mixture onto charred dolomite using microcolumn at different masses of charred dolomite.

Mass of adsorbent	k_T (mL/min µg)	q_0 (µg/g)	R^2
0.5 g	46.5×10^{-3}	87.51	0.989
1 g	32.8×10^{-3}	130.25	0.992
2 g	27.9×10^{-3}	157.89	0.986

process. For a better comparison, the Thomas model was applied to the data obtained in the multicomponent process. Figure 6 shows the applicability of this model to the data. Table 8 shows the calculated values of k_T (Thomas constant) and q_0 (maximum column adsorption capacity). Comparing the results in Table 8 with results in Table 4, it is obvious that the charred dolomite maintained its adsorption capacity for As(V) and As(III) in the multicomponent system, for example, the value of the adsorption capacity obtained in Table 8 for 1 g of charred dolomite was 130.25 µg/g, whereas the value obtained for As(V) onto 1 g of charred dolomite was 137.94 µg/g (see Table 4), and in the case of As(III) onto the same amount of charred dolomite, the adsorption capacity was found to be 127.4 µg/g (see Table 4). The same behaviour was noticed with the values of k_T (adsorption rate constant); the values of k_T for the multicomponent system were in the intermediate region between the values for the As(V)–charred dolomite system and the values for As(III)–charred dolomite system. For example, the value of k_T obtained in Table 8 for 1 g of charred dolomite was 32.8×10^{-3} ml/min µg, whereas the value obtained for As(V) onto 1 g of charred dolomite was 31.3×10^{-3} ml/min µg (see Table 4), and in the case of As(III) onto the same amount of charred dolomite the adsorption capacity was found to be 34.7×10^{-3} ml/min µg (see Table 4). This behaviour is a result of the lack of competition between As(V) and As(III) ions, which can be attributed to the difference in the adsorption mechanism for each one of them onto the charred dolomite. Essentially, it is a monolayer adsorption mainly in case of single As(V) onto charred dolomite, and heterogeneous adsorption mainly in case of single As(III) onto charred dolomite; whereas it appears that each species followed its own mechanism in the binary system.

Figure 7 shows the analysis of the experimental breakthrough data using the BDST equation. BDST data represent the evolution of the bed running time (for different concentrations, C_t = 20%, 40%, 60% and 80%) as a function of the bed depth (Z) based on the experimental data obtained at different masses of adsorbent for adsorption of As(V) and As(III) onto charred dolomite. The BDST parameters: BDST adsorption capacity (N_0) and rate constant (K_a) were calculated from the linearized experimental data and are presented in Table 9, for 20%, 40%, 60% and 80% breakthrough. The linearization of the experimental data using this mathematical model was successful for the adsorption of arsenic onto charred dolomite in a binary system.

It is shown in Table 9 that the adsorption capacity increased as the breakthrough value increased. The calculated values of the adsorption capacities obtained by the BDST model followed the same pattern in the values obtained by Thomas model. These values were found to be between the values for the As(V)–charred dolomite system and the values for As(III)–charred dolomite system at all the breakthrough points (see Tables 4). Table 9 also shows that the adsorption rate constant, K_a, increases as the breakthrough value increased. The service times obtained at 20%, 40%, 60% and 80% breakthrough are illustrated in Table 9. As concluded earlier, the rate of the adsorption process in the binary system was almost as fast as the rate in the case of single arsenic system. As an example, the service time (at 20% breakthrough and 14.9 mm bed depth) for the binary system was 171 min, while at the same circumstances it was 158 min and 161 min for the As(V)–charred dolomite and As(III)–charred dolomite systems, respectively. This observation strengthens the theory that the difference in the adsorption mechanisms for As(V) and As(III) onto the charred dolomite restricted the competition between species; thus, the adsorption process was not affected by the binary mixture.

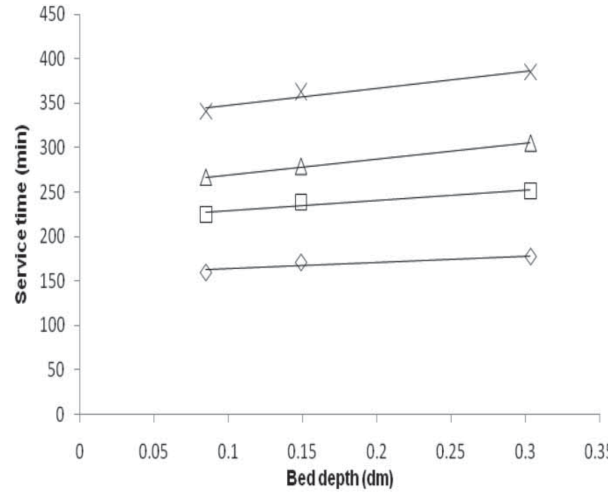

Figure 7. Plots of bed depth (Z) versus service time at different percentage breakthrough points for adsorption of As(V) and As(III) mixture onto charred dolomite (x: 80%, Δ: 60%, □: 40%, ◇: 20%).

Table 9. BDST parameters for the adsorption of As(V) and As(III) mixture onto charred dolomite.

Bed depth (mm)	Service time at breakthrough percentages (min) 20%	40%	60%	80%	N_0 (mg/dm^3)	N_0^a (µg/g)	K_a^b (L/µg min)
					20% ⇒ 40.4	46.70	–
8.50	160	225	267	341	40% ⇒ 62.7	72.45	–
14.90	171	239	279	363	60% ⇒ 95.9	110.84	3.22×10^{-6}
30.35	178	251	304	385	80% ⇒ 104.5	120.81	8.43×10^{-6}

[a] N_0 (µg/g) was calculated by multiplying the value of N_0 (mg/dm^3) by the bulk density.
[b] Values of K_a did not compute for 20% and 40% breakthrough due to their negative values.

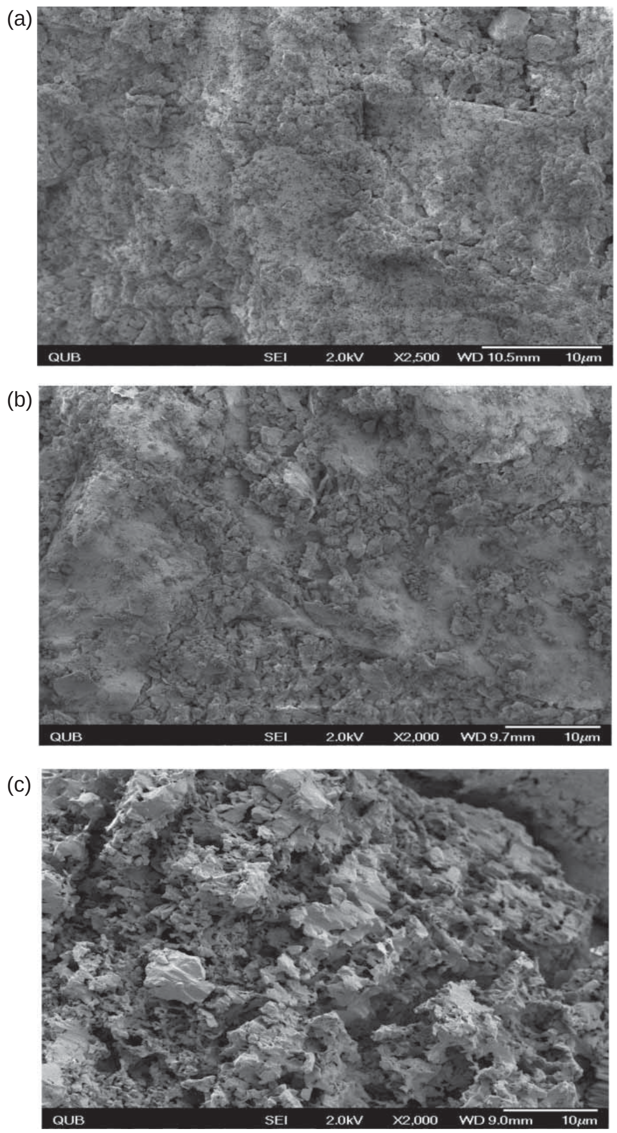

Figure 8. SEM images of charred dolomite at 700 °C for 8 h: (a) before the adsorption process, (b) after the adsorption of As(V) and (c) after the adsorption of As(III).

3.7. SEM images

To characterize the adsorption of arsenic onto charred dolomite, scanning electron microscope (SEM) micrographs of the grain cross-sections were reported. Figure 8(a)–(c) show the SEM images of charred dolomite before and after the adsorption of As(V) and As(III). Figure 8(b) shows the surface of (700 °C, 8 h) charred dolomite after the adsorption of As(V). The surface looks muddy with the presence of some sharp edges and new crystals. Figure 8(a) and (b) proves the formation of new crystals on the surface of the charred dolomite, which implies that the adsorption of As(V) took place on the monolayer of the sample. Figure 8(c) shows the formation of new pores and voids alongside the formation of new crystals on the surface of the charred dolomite. This confirms that the adsorption of As(III) did not only take place in the monolayer of the sample but also in the inner layers.

4. Conclusions

The microcolumn method described here is suitable for speeding up the determination of adsorption parameters of arsenic onto dolomite. This method is inexpensive and can be performed in a few hours instead of few days. On the basis of the experimental results, it can be concluded that the adsorption of As(V) and As(III) onto charred dolomite exhibited a characteristic ‘S’ shape and can be simulated effectively by the Thomas model. It is shown that the adsorption capacity increased as the initial arsenic concentration increased. The increase in the arsenic uptake capacity with the increase of the adsorbent mass in the column was due to an increase in the adsorbent surface area available for the arsenic chemisorptions. A slow decrease in the column adsorption capacity was noticed with an increase in particle size from smaller than 0.335 to 0.710–2.00 mm. For the binary system, the results show that the adsorption of As(V) and As(III) was almost not affected by the presence of both of them in the solution. The experimental data correlated well with the calculated data using the Thomas equation and the BDST equation. Therefore, it might be concluded that the Thomas equation and the BDST equations can produce accurate prediction for various concentrations of arsenic, mass of the adsorbent and the particle size.

References

[1] Lizama K, Fletcher TD, Sun G. Removal processes for arsenic in constructed wetlands. Chemosphere. 2011;84: 1032–1043.
[2] WHO. Guidelines for drinking-water quality. Vol. 4. Geneva: World Health Organization; 2011. p. 315–318.
[3] Mandal B, Suzuki K. Arsenic round the world: a review. Talanta. 2002;58:201–235.
[4] Shao W, Li X, Cao Q, Luo F, Li J, Du Y. Adsorption of arsenate and arsenite anions from aqueous medium by using metal (III)-loaded amberlite resins. Hydrometallurgy. 2008;91:138–143.
[5] Budinova T, Savova D, Tsyntsarski B, Ania CO, Cabal B, Parra JB, Petrov N. Biomass waste-derived activated carbon for the removal of arsenic and manganese ions from aqueous solutions. Appl Surf Sci. 2009;255:4650–4657.
[6] Li Z, Beachner R, McManama Z, Hanlie H. Sorption of arsenic by surfactant-modified zeolite and kaolinite. Micropor Mesopor Mater. 2007;105:291–297.
[7] Yusof AM, Malek NA. Removal of Cr(VI) and As(V) from aqueous solutions by HDTMA-modified zeolite Y. J Hazard Mater. 2009;162:1019–1024.
[8] Kundu S, Gupta A. Arsenic adsorption onto iron oxide-coated cement (IOCC): regression analysis of equilibrium data with several isotherm models and their optimization. Chem Eng J. 2006;122:93–106.
[9] Guan X, Wang J, Chusuei CC. Removal of arsenic from water using granular ferric hydroxide: macroscopic and microscopic studies. J Hazard Mater. 2008;156:178–185.

[10] Biswas BK, Inoue J, Inoue K, Ghimire KN, Harada H, Ohto K, Kawakita H. Adsorptive removal of As(V) and As(III) from water by a Zr(IV)-loaded orange waste gel. J Hazard Mater. 2008;154:1066–1074.
[11] Kim S, Lee W, Cho H, Lee B, Lee P, Choi S. Equilibria, kinetics, and spectroscopic analyses on the uptake of aqueous arsenite by two-line ferrihydrite. Environ Technol. 2014;35:251–261.
[12] Baltazar S, García A, Romero A, Rubio M, Arancibia-Miranda N, Altbir D. Surface rearrangement of nanoscale zerovalent iron: the role of pH and its implications in the kinetics of arsenate sorption. Environ Technol. 2014 (in press).
[13] Jaafarzadeh N, Amiri H, Ahmadi M. Factorial experimental design application in modification of volcanic ash as a natural adsorbent with Fenton process for arsenic removal. Environ Technol. 2012;33:159–165.
[14] Prasad K, Ramanathan A, Paul J, Subramanian V, Prasad R. Biosorption of arsenite (As^{+3}) and arsenate (As^{+5}) from aqueous solution by *Arthrobacter* sp. biomass. Environ Technol. 2013;34:2701–2708.
[15] Wu S, Hu W, Luo X, Deng F, Yu K, Luo S, Yang L, Tu X, Zeng G. Direct removal of aqueous As(III) and As(V) by amorphous titanium dioxide nanotube arrays. Environ Technol. 2013;34:2285–2290.
[16] Albadarin AB, Mangwandi C, Al-Muhtaseb AH, Walker GM, Allen SJ, Ahmad MNM. Kinetic and thermodynamics of chromium ions adsorption onto low-cost dolomite adsorbent. Chem Eng J. 2012;179:193–202.
[17] Karaca S, Gurses A, Ejder M, Acikyildiz M. Adsorptive removal of phosphate from aqueous solutions using raw and calcinated dolomite. J Hazard Mater. 2006;B128:273–279.
[18] Walker G, Hanna JA, Allen SJ. Treatment of hazardous shipyard wastewater using dolomitic sorbents. Water Res. 2005;39:2422–2428.
[19] Duffy A, Walker G, Allen SJ. Investigations on the adsorption of acidic gases using activated dolomite. Chem Eng J. 2006;117:239–244.
[20] Boucif F, Marouf-Khelifa K, Batonneau-Gener I, Schott J, Khelifa A. Preparation, characterisation of thermally treated Algerian dolomite powders and application to azo-dye adsorption. Powder Technol. 2010;201:277–282.
[21] Al-Degs YS, El-Sheikh AH, Al-Ghouti MA, Hemmateenejad B, Walker GM. Solid-phase extraction and simultaneous determination of trace amounts of sulphonated and azo sulphonated dyes using microemulsion-modified-zeolite and multivariate calibration. Talanta. 2008;75:904.
[22] Walker GM, Weatherley LR. COD removal from textile industry effluent: pilot plant studies. Chem Eng J. 2001;84:125–131.
[23] Duffy A, Walker GM, Allen S. Investigations on the adsorption of acidic gases using activated dolomite. Chem Eng J. 2006;117:239–244.
[24] Albadarin AB, Mangwandi C, Al-Muhtaseb AH, Walker GM, Allen SJ, Ahmad MNM. Modelling and fixed bed column adsorption of Cr(VI) onto orthophosphoric acid-activated lignin. Chinese J Chem Eng. 2012;20:469–477.
[25] Rozada F, Otero M, García AI, Morán A. Application in fixed-bed systems of adsorbents obtained from sewage sludge and discarded tyres. Dyes Pigm. 2007;72:47–56.
[26] Walker GM, Weatherley LR. A simplified predictive model for biologically activated carbon fixed beds. Process Biochem. 1997;32:327–335.
[27] Al-Ghouti M, Khraisheh M, Ahmad MNM, Allen SJ. Micro-column studies of dye adsorption onto manganese oxides modified diatomite. J Hazard Mater. 2007;146:316–327.
[28] Salameh Y, Al-Lagtah N, Ahmad MNM, Allen SJ, Walker GM. Kinetic and thermodynamic investigations on arsenic adsorption onto dolomitic sorbents. Chem Eng J. 2010;160:440–446.